Technobius Physics, 2024, 2(3), 0015, https://doi.org/10.54355/tbusphys/2.3.2024.0015

Technobius Physics

https://technobiusphysics.kz/

e-ISSN 3007-0147

Corrigendum Notice: A corrigendum has been issued for this article and is included at the end of this document.

Article

Exploring particle physics through diffusion chambers: detecting, visualizing, and analyzing subatomic phenomena

Dastan Zhumanov[1,*], Cholpon Maripova[2]

[1]Satbayev University, Institute of Automation and Information Technologies, 22a Satpaev Str., Almaty, Kazakhstan
[2]Kyrgyz State Technical University, Department of Physics, 66, Ch.Aitmatov Ave., Bishkek, Kyrgyzstan
*Correspondence: dastan.zhumanov.02@mail.ru

Abstract. This study examines the development and utilization of diffusion chambers in particle physics research. Through meticulous experimentation, optimization of chamber parameters has been achieved to enhance particle detection while concurrently assessing background radiation levels, vital for minimizing interference. Furthermore, recent advancements have enabled the visualization of α – particles and mesons within these chambers, offering invaluable insights into their behaviors and interactions. These achievements highlight the pivotal role of diffusion chambers as indispensable tools in advancing our understanding of fundamental particles and their properties. As a result, diffusion chambers continue to serve as critical instruments in unraveling the mysteries of the subatomic world, promising continued contributions to particle physics research.
Keywords: diffusion chambers, particle physics, background radiation, α – particles, mesons.

1. Introduction

1.1 Cosmic radiation

High intensity particle radiations (photon rays being an example, since they are electromagnetic waves) usually come from space and penetrate all layers of the Earth's atmosphere (called main cosmic radiations). These radiations' principal constituents are as follows: protons (approx. 90%), α – particles (approx. 9%), bigger nuclei (up to 1%) [1].

Particles often clash with atmospheric nuclei as they pass through the atmosphere, starting fission and nuclear reactions. As a result, fresh nuclei and fundamental particles are created, continuing on their current path and triggering other interactions [2].

There is only one detectable secondary form of radiation in the atmospheric layers closest to the Earth's surface (below 20 km), which originates from the many interaction processes occurring in the upper atmospheric layers [3].

It thus becomes necessary to differentiate between four different parts, each with a different penetration strength. Table 1 gives information on the detailed composition of the components [2], [3], [4].

Table 1 – Components of the cosmic secondary rays

Cosmic secondary rays	Components
Nucleons	Protons / neutrons
Electrons and photons	Electrons / positrons / photons
Mesons	Mesons of different charges
Neutrinos	Neutrinos / antineutrinos

Figure 1 schematically illustrate the expansion process of secondary cosmic ray components.

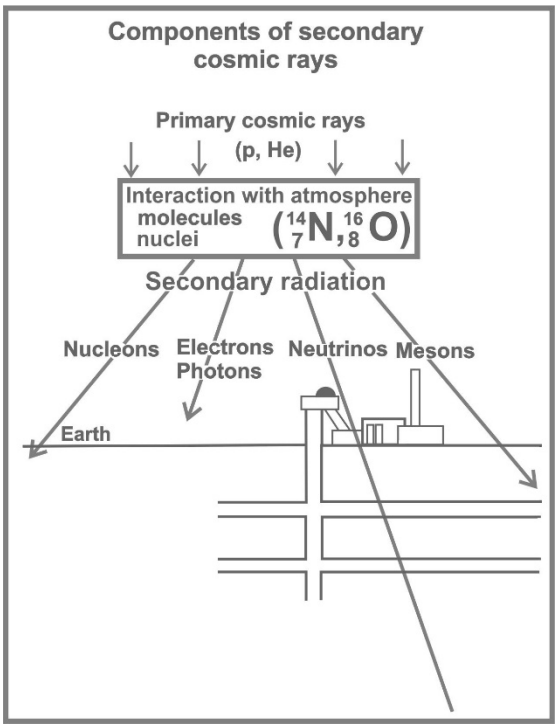

Figure 1 – Organic division mechanisms

All electrically charged particles, such as protons, electrons, positrons, mesons, and alpha particles, can be found inside the special equipment [5]. On the other hand, photons only produce an indirect trace when they, for example, remove an electron from an atom, leaving behind an ionization trail. Because neutrons can initiate nuclear reactions, they cause traces to be formed through the charged particles that are released from the nucleus. Table 2 summarizes the components of the trace that is left behind by the nuclear reactions of neutrons [6].

Table 2 – The trace that is left behind by the nuclear reactions of neutrons

Particles	Symbol	Relative mass	Charge	Radioactive period
Electron	e^-	1	-1	Stable
Positron	e^+	1	+1	Stable
Myon	μ^-	206.77	-1	$1.5 * 10^{-6}$s
Antimyon	μ^+	206.77	+1	$1.5 * 10^{-6}$s
Proton	p^+	1836.1	+1	stable
Neutron	n	1836.62	0	14.7 min
α – particle	He^{++}	7294.1	+2	Stable

1.2 Radiations from the earth (Terrestrial)

Natural radionuclides that emit radiation are present in all elements on Earth, including the atmosphere, water, animals, and soil [7], [8]. They have either always existed or have been created since the Earth's creation, which is approximately 4.5 billion years ago: Among the naturally occurring radionuclides are U-238, Th-232, K-40, and Rb-87, which have extremely long radioactive periods [8]. There is a continuous production of Ra-226, Rn-222, Po-218, or Pb-210, radionuclides with relatively short radioactive periods in the three natural splitting processes. Naturally occurring radionuclides with comparatively short radioactive periods do exist, but they are not involved in the splitting process. In the highest layers of the atmosphere, they are continuously being formed. For example, C-14 from N-14 or H-3 from N-14 or O-16.

There are roughly 100 naturally occurring radionuclides in the Earth's crust, all of which exist in varying amounts and have existed since the planet's formation. This explains the continuous exchanges that occur between the atmosphere, water, earth, and animal life (Figure 2).

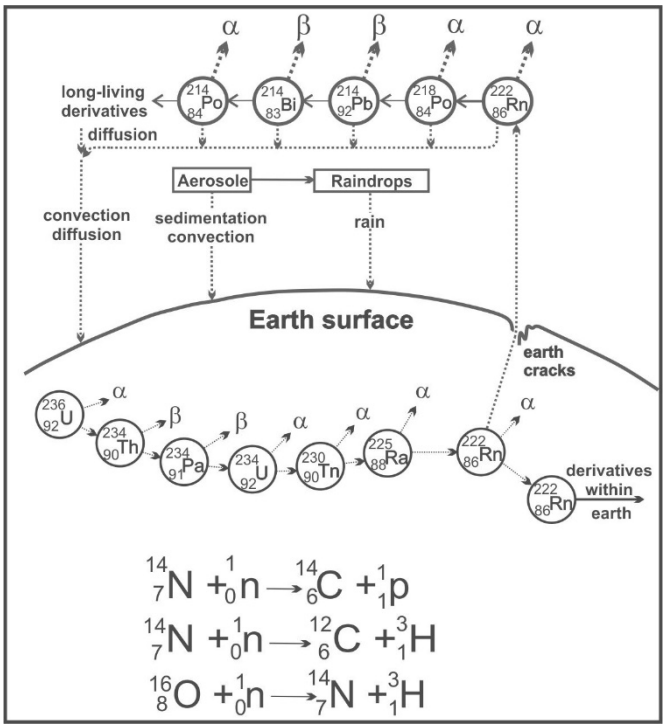

Figure 2 – Production of Rn-222 and derivatives in the low atmosphere layer

As it is known, not a few researches have been carried out in the field of creation of diffusion chambers for observation of charged particle tracks [9]. Some scientists [10] conducted experiments to determine the most suitable materials for making a diffusion chamber. They tested different substances to assess their compatibility with particle track detection and visualisation. Factors such as transparency, durability and sensitivity to ionisation were evaluated. Through systematic testing and comparison, materials such as glass or plastic were identified as having optimal characteristics for use in the chamber, but the sensitivity of the chamber was not ideal.

Other researchers [11] have explored different camera configurations and geometries to improve particle detection and track visualisation. They experimented with camera sizes, shapes and detection element locations to maximise sensitivity and resolution. By systematically changing these parameters and analysing the resulting particle tracks, they were unable to improve the camera design to achieve optimal performance.

The team of scientists [12] conducted extensive research to determine the ideal operating conditions for the diffusion chamber. They adjusted parameters such as temperature, pressure and gas composition to optimise particle detection efficiency and track visibility.

Through systematic experimentation and data analysis, they determined the optimal range of operating parameters that facilitated the most accurate and reliable observation of particle tracks in the chamber.

Consequently, there arises a necessity to devise a chamber constructed from naturally occurring radioactive elements.

2. Methods

A special diffusion chamber was constructed for the experiment, which consisted of a chamber base and an observation chamber, the two main parts of the cloud chamber device. The camera base includes a pump, a programmable time switch, a power supply, a cooling mechanism

and an alcohol reservoir. The surveillance camera is attached to this base. At the bottom of the surveillance camera is a large black metal panel measuring 45 by 45 cm, which is continuously cooled to a temperature of about -30°C using a cooling device (Figure 3).

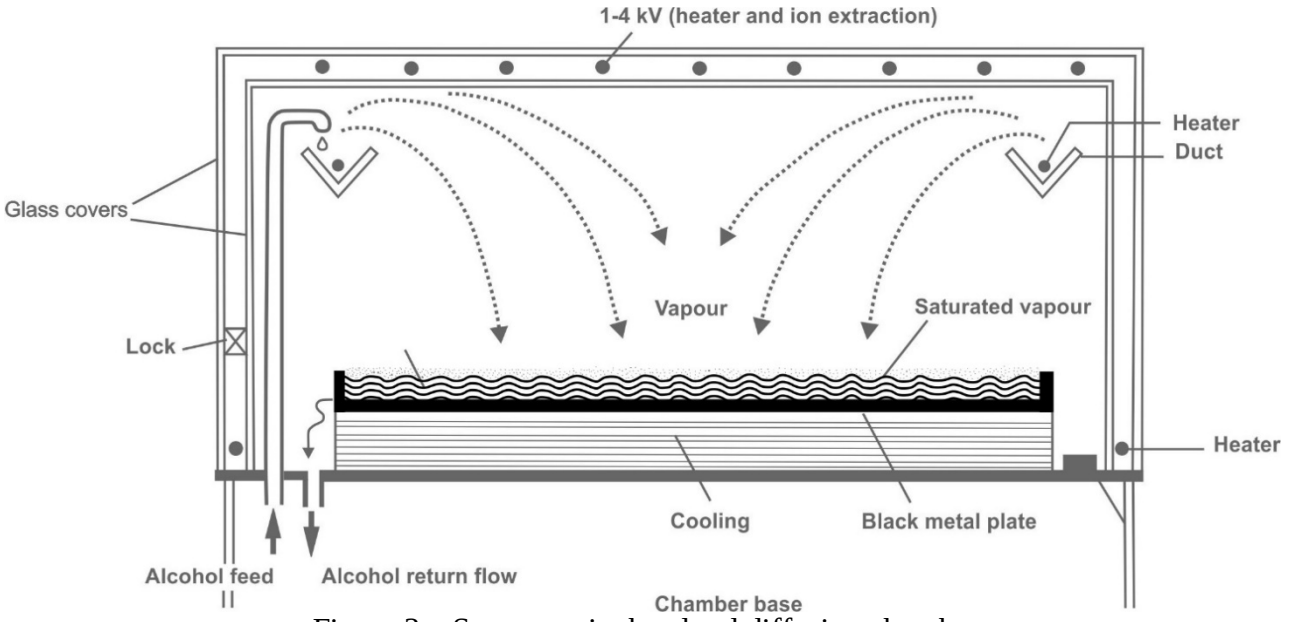

Figure 3 – Segment via the cloud diffusion chamber

The surveillance camera consists of two folded glass covers for the side and top plates. A system of tiny heating wires is located inside this structure between the upper glass panels to prevent condensation inside the hood. These wires are simultaneously under high voltage, which generates an electric field that attracts ions. A heated trough surrounding the entire top of the glass hood is powered by electricity. A curved tube supplies isopropyl alcohol, which flows into the trough. The alcohol moves from the warmer upper part of the chamber to the cooler lower part, where it evaporates and dissipates, then condenses into tiny droplets and returns to the tank. Just above the thin layer of liquid covering the bottom, a region of supersaturated alcohol vapour forms. This region is the only place where charged particles from internal or external sources create ions as they pass through it. Tiny droplets of alcohol cling to these ions, creating a visible cloud track. The length and location of this track gives information about the composition of the ionising particles.

The designed chamber was placed on a square table with a length of 90 to 100 cm and a height of 30 to 60 cm. Throughout the experiment, the cloud chamber was fully shielded from direct overhead light and the vents were not obstructed. For best observing conditions, the entire experiment took place in the dark.

Protons, mesons, electrons, and alpha particles — all of which have an electrical charge— record the tracks left by this diffusion chamber. You may determine which particle passed through the cloud chamber, how fast it traveled (energy), and whether it collided or deflected during flight by observing the differences in the particle's trails. The alcohol vapor that is diffusing to the black plate from top to bottom liquefies (condenses into droplets) as soon as it gets close to the cooled plate.

There is a layer of liquid alcohol vapour, about 1-2 mm thick, above which the vapour has not completely liquefied. Drop formation, and hence cloud formation, can be intentionally induced in this layer by, for example, small dust particles (condensation nuclei) or passing radiation particles. Radiation particles "damage" (ionize) many alcohol molecules during flight; these molecules can then take on considerably larger alcohol droplets and appear visible to us. On Figure 4, they form the cloud track.

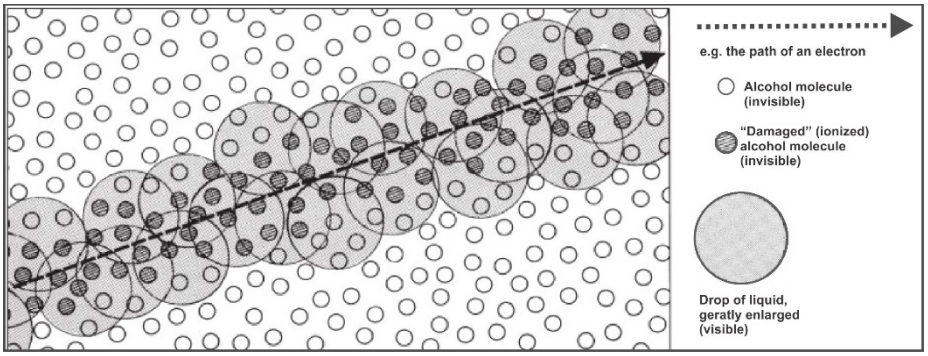

Figure 4 – Cloud chamber: the formation of cloud tracks

The first white tracks on the black surface appeared five minutes after the start of work. To maintain high accuracy and sensitivity, the temperature inside the chute was increased.
The readings of the programmable timer were set to the automatic mode of operation of the cloud camera. In addition, the base of the camera was equipped with a hole in which artificial radiation sources are supposed to be inserted.

To ensure the reliability of observations and confirm the accuracy of data, statistical processing principles were applied to each measurement:

- before starting measurements, the start time of track visualization was recorded and preliminary calibration of conditions (temperature, lighting, evaporation stability) was performed.
- a method was used that mimicked the operation of a geiger counter—a sheet of paper with a hole 0.8 cm in diameter, through which multiple visual counts of the number of tracks were made over a given time interval.
- each measurement was repeated at least five times, and the track frequency values in the observation area were recorded.
- based on these observations, the mean values (m) and standard deviation (σ) were calculated using the formula:

$$\sigma = \sqrt{\frac{1}{n-1}\sum_{i=1}^{n}(x_i - M)^2} \quad (1)$$

Where, σ — standard deviation: numerically shows how much individual measurements deviate from the mean value. The smaller σ is, the higher the accuracy and stability of measurements; n — total number of measurements (observations), i.e., how many times you counted the number of particles during the same time interval; x_i — value i of the i-th measurement, i.e., the number of particles recorded in the i-th attempt; M — arithmetic mean (mathematical expectation) for all measurements; $(x_i - M)^2$ — the square of the deviation of each measurement from the mean value. Squaring is done so that the deviations do not cancel each other out (since some of them are negative); $\sum_{i=1}^{n}(x_i - M)^2$ — sum of squares of all deviations. This is a measure of the overall "scatter" of the data; $\frac{1}{n-1}$ — a forming coefficient called the unbiased estimate of variance. Division by n−1 (rather than n) is used to correctly approximate the actual standard deviation if the sample size is finite (the so-called "unbiased estimate").

The obtained values were compared with the theoretical background radiation level (about 18 events per minute), which made it possible to identify excesses caused by artificial or cosmic sources.

In addition, the length, shape, and density of droplets along the track served as indirect statistical indicators for classifying particles (alpha, beta, muons, etc.). Tracks were divided according to length (short/long), droplet density (dense/sparse), and shape (straight/curved) for visual identification of the energy and type of particles.

In the future, it is planned to expand the statistical component using digital video recording and subsequent analysis of tracks using software with elements of machine vision and automatic tracking.

3. Results and Discussion

Unless they are separated in a carefully insulated environment, the radioactive particles described in the previous section will always be present as background radiation. When radioactive events like decay are being studied, it is necessary to subtract the background radiation, which is usually measured at about 18 rpm, from the observed effects. Removing this amount is necessary for a precise analysis. Traditionally, this background radiation is measured using a tube counter connected to a counting device. But upon first examination of the cloud chamber's active region, a seemingly profusion of particle tracks would indicate that radioactive material—rather than just background radiation—is present in the chamber. A modest method is used to help identify background radiation as the true source of the particle track density.

Using a piece of type paper, hole in the middle of it that is about 0.8 cm in diameter to replicate the operation of a tube counter have been made. Lay the paper out flat on the cloud chamber's glass plate. Using one eye, look through the hole to the active part of the cloud chamber at a distance of about 10 cm from the paper. Count the twenty different "parts" of particle tracks that are visible through the hole and record the elapsed time at the same time.

This method simulates a tube counter's aperture. Particle tracks are only visible where they intersect this imagined opening. Out of all the particle trails in the cloud chamber, only those passing through a tube counter-like aperture are visible. This technique can verify the theoretical zero rate of particle detection. Observable are remnants of "clouds" made up of protons, electrons/positrons, mesons, and particles within the chamber. Short tracks and longer, narrower tracks are often visible. For now, we will concentrate on the longer but more noticeable tracks (Figure 6).

The tracks are statistically dispersed over the observation region, making it impossible to forecast the exact time and place of future track sightings. α – particles in air conditions usually have a diameter of around 5 cm, but in alcohol vapor, their range is significantly reduced. Moreover, α – particles can be absorbed by a single sheet of paper.

On the one hand, the decay of a radioactive nucleus might release α – particles inside the chamber. On the other hand, it is possible that protons—which have a lot of energy—are produced in the atmosphere during secondary radiation processes. These powerful protons are able to pass past the glass shielding and inside the chamber. Then, when they enter the chamber, if their energy is low enough to interact with the atomic electrons of the gas inside, they leave behind α – particles like tracks (Figure 7).

Figure 6 – Track produced by an α – particle

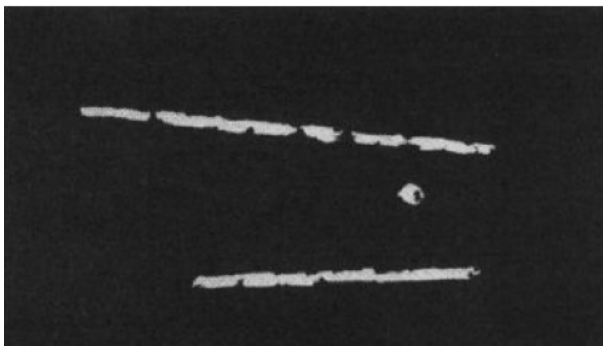

Figure 7 – Track produced by protons

The supersaturated alcohol vapor layer only permits the identification of a single location as an ionization trail when it is penetrated vertically. When the observer directs attention towards the thin and, to some extent, significantly elongated tracks (tracks exhibiting low drop density), a notable abundance of track manifestations may cause perplexity. Therefore, it is recommended to meticulously consider specific characteristics—namely, the length of these tracks.

Primarily, observers should endeavor to identify a thin, linear, and prolonged trajectory extending across the entire observation area. This trajectory is indicative of particularly swift

electrons (Figure 8). Conversely, electrons moving at a slower pace (i.e., possessing a lower energy content) exhibit shorter trajectories, which are partially curved or distorted (Figure 9) due to deviation.

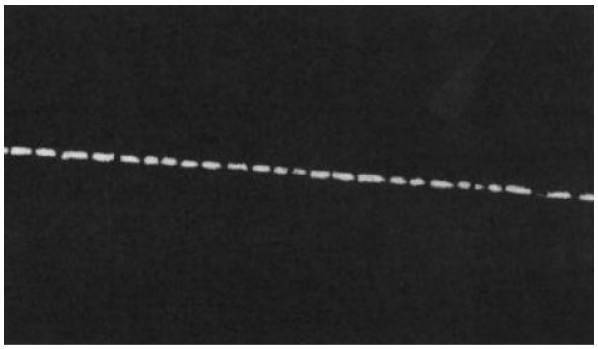

Figure 8 – A track produced by an electron having a high energy content

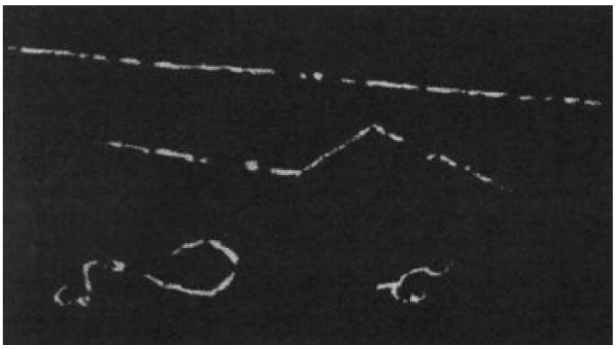

Figure 9 – Repeatedly deviating β-particles create a track

Because of the numerous atoms' deviations in the steam layer, electrons with very low energy content produce short trajectories that appear ornate or convoluted (Figure 10).

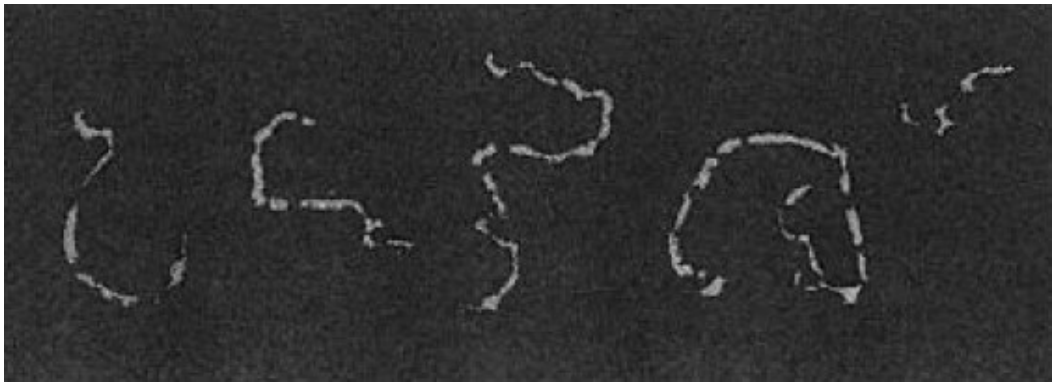

Figure 10 – Tracks made up of β - particles with less energy

When beta β-particles with low energy pass through a diffusion chamber, they ionize the supersaturated alcohol vapor above the thin liquid layer at the bottom, resulting in short, ornate, or convoluted tracks. These tracks are distinctive due to the numerous deviations and interactions the low-energy β-particles experience with atoms in the vapor layer. The short length of these tracks indicates the lower energy of the particles, while the convoluted appearance reflects the frequent scattering events they undergo. These visible trails, formed within the carefully controlled environment of the chamber, provide valuable information about the energy and behavior of β-particles. The intricate nature of the tracks aids in distinguishing low-energy β-particles from other types of ionizing particles, offering insights into their interactions and properties.

In the Cloud chamber, mesons—which make about 90% of secondary cosmic rays—can also be found. Because m-mesons have an elementary charge that can be either positive or negative and because their weight is equivalent to 207 times that of an electron, they play a significant role in this process. High energy mesons produce trajectories that resemble the tracks left by electrons. On the other hand, heavily regulated mesons ionize and create tracks that are almost exactly like those of - particles. As a result, it will be exceedingly challenging to determine if one is looking at protons, electrons, mesons, or particles in a given instance (Figure 11).

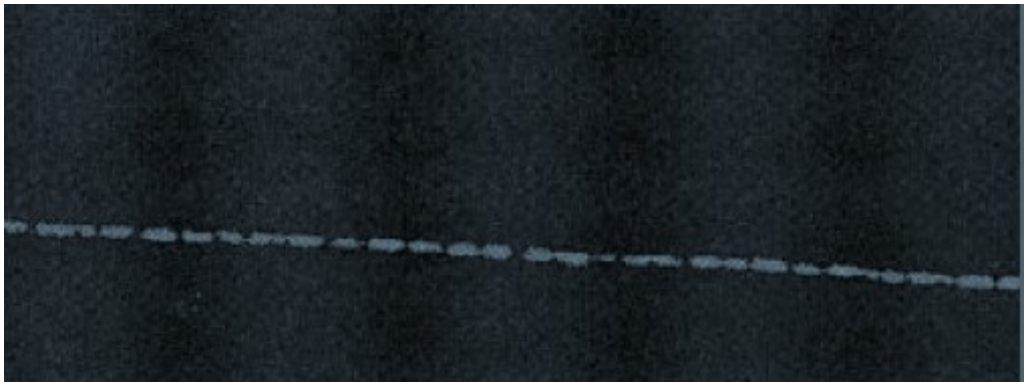

Figure 11 – Track produced by a meson

When a meson passes through a diffusion chamber, it ionizes the supersaturated alcohol vapor just above the thin liquid layer at the bottom, creating a visible cloud track. This track, characterized by its intermediate length and narrower width compared to heavier particles like alpha particles, allows for detailed analysis. The track's curvature provides insight into the meson's momentum and energy, while any bends or kinks can indicate collisions or deflections. Additionally, the meson's inherent instability might be observed through sudden changes in the track, marking decay events. These visible trails, formed within the controlled environment of the chamber—shielded from direct light and regulated for temperature and voltage—offer valuable data for identifying the meson and understanding its interactions and properties.

4. Conclusions

In conclusion, it should be noted that the development and improvement of diffusion chambers have become important milestones in research in the field of particle physics. Thanks to careful experiments, it was possible not only to optimize the camera parameters to improve particle detection, but also to conduct a thorough assessment of background radiation levels. This definition is important to minimize interference and ensure the accuracy of particle observations. Moreover, recent advances have made it possible to visualize α – particles and masons inside these chambers, shedding light on their behavior and interactions in ways previously unattainable. These achievements highlight the crucial role of diffusion chambers as indispensable tools in uncovering the mysteries of the subatomic world and deepening our understanding of fundamental particles and their properties.

References

[1] R. A. Millikan, “History of research in cosmic rays,” *Nature*, vol. 126, no. 3166, 1930, doi: 10.1038/126014A0.

[2] R. A. Millikan, “Remarks on the history of cosmic radiation,” *Science (80-.).*, vol. 21, no. 1851, pp. 640–641, Jun. 1930, doi: 10.1126/SCIENCE.71.1851.640/ASSET/CA7999E5-1117-40F6-AAC9-C8FCDEA52D81/ASSETS/SCIENCE.71.1851.640.FP.PNG.

[3] K. G. McCracken, “Variations in the Cosmic-Ray Rigidity Spectrum,” *Phys. Rev.*, vol. 113, no. 1, p. 343, Jan. 1959, doi: 10.1103/PhysRev.113.343.

[4] F. B. McDonald, “Primary Cosmic-Ray Intensity near Solar Maximum,” *Phys. Rev.*, vol. 116, no. 2, p. 462, Oct. 1959, doi: 10.1103/PhysRev.116.462.

[5] A. Bertelsmann and R. H. Heist, “Nucleation of 1-Pentanol Using a Thermal Diffusion Cloud Chamber,” *Aerosol Sci. Technol.*, vol. 28, no. 3, pp. 259–268, Jan. 1998, doi: 10.1080/02786829808965526.

[6] N. Schaeffer, F. Utheza, F. Garnier, and G. Lauriat, “Stable stratification alteration in a thermal diffusion cloud chamber,” *J. Chem. Phys.*, vol. 113, no. 18, pp. 8085–8092, Nov. 2000, doi: 10.1063/1.1315358.

[7] F. A. Abd El-Salam and L. Sehnal, “The effects of the terrestrial infrared radiation pressure on the earth’s artificial satellite dynamics,” *Appl. Math. Comput.*, vol. 162, no. 3, pp. 1431–1451, Mar. 2005, doi: 10.1016/J.AMC.2004.03.019.

[8] D. Jones, “Terrestrial myriametric radiation from the earth’s plasmapause,” *Planet. Space Sci.*, vol. 30, no. 4, pp. 399–410, Apr. 1982, doi: 10.1016/0032-0633(82)90046-0.

[9] R. H. Heist, A. Kacker, and J. Brito, “NUCLEATION AND GROWTH IN THE DIFFUSION CLOUD CHAMBER II STEADY STATE NUCLEATION,” *Chem. Eng. Commun.*, vol. 28, no. 1–3, pp. 117–125, Jun.

1984, doi: 10.1080/00986448408940126.
[10] F. T. Ferguson, R. H. Heist, and J. A. Nuth, "Vapor transport within the thermal diffusion cloud chamber," *J. Chem. Phys.*, vol. 113, no. 17, pp. 7398–7405, Nov. 2000, doi: 10.1063/1.1312381.
[11] R. H. Heist, A. Bertelsmann, D. Martinez, and Y. F. Chan, "Thermal diffusion cloud chamber: new criteria for proper operation," *Atmos. Res.*, vol. 65, no. 3–4, pp. 189–209, Jan. 2003, doi: 10.1016/S0169-8095(02)00149-7.
[12] J. Smolík and J. Vašáková, "Experimental Study of Thermodiffusiophoresis By Use of a Thermal Diffusion Cloud Chamber," *Aerosol Sci. Technol.*, vol. 14, no. 4, pp. 406–417, Jan. 1991, doi: 10.1080/02786829108959502.

Dastan Zhumanov – Master Student, Satbayev University, Institute of Automation and Information Technologies, 22a Satpaev Str., Almaty, Kazakhstan, dastan.zhumanov.02@mail.ru
Cholpon Maripova – Master Student, Kyrgyz State Technical University, Department of Physics, 66, Ch.Aitmatov Ave., Bishkek, Kyrgyzstan, cholpon.maripova@mail.ru

Author Contributions:
Dastan Zhumanov – concept, methodology, resources, data collection, testing, modeling.
Cholpon Maripova – analysis, visualization, interpretation, drafting, editing, funding acquisition.

Received: *13.05.2024*
Revised: 30.06.2024
Accepted: 08.07.2024
Published: 09.07.2024

Conflict of Interest. The authors declare no conflict of interest.

Use of Artificial Intelligence (AI): The authors declare that AI was not used.

Technobius Physics, 2024, 2(3), 0015c, https://doi.org/10.54355/tbusphys/2.3.2024.0015c

Technobius Physics

https://technobiusphysics.kz/

e-ISSN 3007-0147

Corrigendum Notice: A corrigendum has been issued for this article and is included at the end of this document.

Post-Publication Notice

Corrigendum to "D. Zhumanov and Ch. Maripova, "Exploring particle physics through diffusion chambers: detecting, visualizing, and analyzing subatomic phenomena", tbusphys, vol. 2, no. 2, p. 0015, Jul. 2024. doi: 10.54355/tbusphys/2.2.2024.0015"

In the originally published version of this article, the Methods section lacked details on the statistical processing of measurements used to validate observation reliability. The following corrections have been made:

1. Section 2 (Methods):

- The updated version specifies preliminary calibration steps, repeated measurements (n=5), mean value (m) and standard deviation (σ) calculation formulas, and comparison with theoretical background radiation level (18 events/min).

- Visual classification of tracks (length, density, curvature) is now described as an additional indirect indicator of particle type and energy.

- A note on future enhancements using digital video recording and machine vision for automatic track analysis has been added.

2. Editorial improvements were made to enhance methodological transparency and reproducibility of experimental data.

These corrections do not alter the findings, discussion, or conclusions of the article but strengthen the rigor and accuracy of reported measurements.

Published: 19.07.2024